Analysis of Capacitively Driven Electromagnetic Coil Guns

Y. BENCHEIKH, Y. OUAZIR and R. IBTIOUEN

Abstract **-- In this paper, the performance analysis of two stages linear induction launcher (LIL) is presented. It is carried out based on current filament model (CFM) taking their transient behavior into account.**

A computer simulation based on the developed model, is down for predicting the electromechanical characteristics of the launcher (Current, velocity force, etc.). The section to section transitions which have significant effects on the launcher performance are also studied. Some simulation results are presented and discussed.

Index Terms**—Coil Gun, current filament model, Linear induction launcher, Eddy currents.**

I. INTRODUCTION

THE capacitively linear induction launcher (LIL) consists to two principal parts: the barrel coils, energized by discharging capacitors through the coils so as to create a traveling wave; and the projectile, consisting of a thin-walled aluminum cylinder (sleeve). The capacitance values are chosen to resonate with the inductance of the coils at a frequency which increases along the barrel.

Propelling and centering forces are created, simultaneously, by the interaction between the traveling wave magnetic field and the system of currents induced into the sleeve. The increase in frequency is obtained stepwise by dividing the barrel into sections which are energized sequentially [1]-[2]-[3], and this results in a reduction of the number of capacitors and switches.

Somme models are developed for modeling the coaxial accelerators [4]-[5]-[6]-[7]. It has been found that the use of current filament method is the most tools to predict the LIL performances.

In this paper a current filament model is used for the transient behavior analysis of the linear induction launcher powered by capacitors bank. A computer simulation results based on this model are presented and discussed.

II. CURRENT FILAMENT MODEL

Two types of model are usually used for modeling the linear induction launcher: current sheet model [8]-[9] and current filament model (CFM) [10]. The current sheet model is used for the design and steady states analysis, where the transient phenomenon analysis is not necessary. In this model the currents in the coils and projectile are replaced with two equivalent current sheets located at their equivalent radius; by computing the magnetic field produced, the Lorentz force applied on projectile can be obtained. The CFM model is suitable for both transient and steady states operation conditions. This model consists to replace the LIL with an electrical coupled circuit whose parameters are determined analytically. The current filament model divides massive conductive parts of the system into elementary volume elements, in which uniform distribution of current is assumed [11]. An electrical circuit is associated with every volume element. The global electrical and mechanical equations governing the behaviors of the LIL are formulated on the basis of the adopted equivalent network.

A. Basic Model

The coil launcher shown in the Fig. 1 is modelled by the equivalent circuit shown in Fig. 2. Because the axial distribution of the induced current in the sleeve is not uniform, to simulate the physical system we divide the sleeve into the several zones that are electrically insulated from each other and represent them as separate projectile coils. The number of drive coils depends on performance specifications such as the muzzle velocity, weight of the projectile, the calibre, and the length of the barrel. We denote by d the number of drive coils, and by p the number of projectile coils. Employing Kirchhoff's voltage law, we write the network equations in matrix form:

$$[V]=[R][I]+\frac{d}{dt}\{[L][I]+[M][I]\} \tag{1}$$

where $[V]$ and $[I]$ are voltages and currents vector ($m+n$ element) of the individual projectile and drive-coil respectively (Fig.2); $[R]$, $[L]$ and $[M]$ are respectively the resistance, self-inductance and mutual inductance matrices of the equivalent circuit. The formulas used to evaluate each element of $[L]$ and $[M]$ are given in [12]. It should be noted that the mutual inductances $[M]$ between drive coils and projectile coils depends in the projectile position (z) and time, then (1) is rewritten as:

$$\{[L]+[M]\}\frac{d}{dt}[I]=[V]-[R][I]-v_p[G][I] \tag{2}$$

Where v_p is the velocity of the projectile.

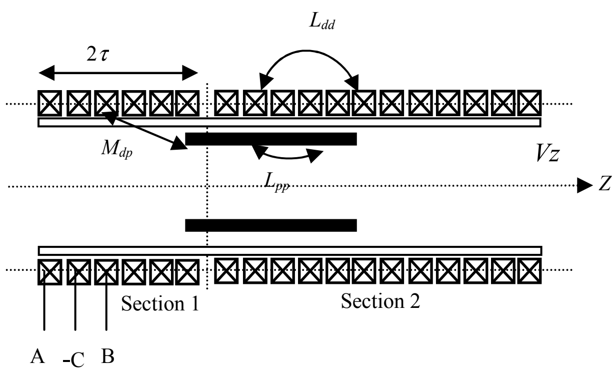

Fig.1. Arrangement of two section induction coil launcher

Y. Bencheikh and Y. Ouazir is with USTHB University laboratoire des systems électriques industriels PB N° 32 El-Alia Bab-Ezzouar 16111 Alger, Algérie. (E-mail: y_bencheikh@yahoo.fr, E-mail: youazir@yahoo.fr).

R.Ibtiouen is with the ENP Alger Laboratoire d'Electrotechnique BP 182 El-Harrach 16200 Alger Algérie (E-mail: ribtiouen@yahoo.com).

978-1-4244-4175-4/10/$25.00 ©2010 IEEE

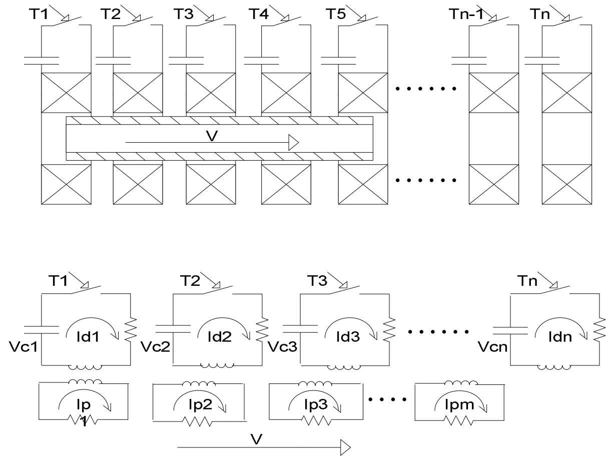

Fig.2. Current filament model of the capacitively driven coil launcher

Knowing that the drive coils are fed through capacitors, the capacitor voltages $[V_c]$ and drive-coil currents $[I_d]$, which are sub matrices of $[V]$ and $[I]$, are related by:

$$[C]\frac{d}{dt}[V_c] = -[I_d] \tag{3}$$

where $[C]$ is a diagonal (d element) matrix containing the capacitances. The Lorentz force acting on the projectile is given by:

$$F = \frac{1}{2}[I]^T[G][I] \tag{4}$$

where $[G]=d[M]/dz$ and the superscript T stands for the transpose of the matrix. Finally, we consider the equation of motion combined with (4) leads to:

$$M_p \frac{dv_p}{dt} = \sum_{p=1}^{m}\sum_{d=1}^{n} I_p I_d \frac{dM_{pd}}{dz} \tag{5}$$

Where M_p and M_{pd} are the mass of projectile and the square (m+n)x(m+n) matrix of mutual inductances between any two individual coils respectively.
The velocity v_p is given by:

$$v_p = \frac{dz}{dt} \tag{6}$$

The complete set of equations which describe the capacitively driven coil-launcher is then given by (2), (3), (5) and (6). These equations represent a set of simultaneous nonlinear differential equations with time variable coefficients. The number of first-order differential equations involved in the system is ($N=2n+m+2$).

III. Numerical Results and Discussion

A capacitively driven two-section coil launcher which is currently being build is used as an example. The dimensions of the launcher are given in Table I. A two-section barrel with a total length of 60 cm was designed to accelerate a 127g Aluminum projectile. The muzzle velocity of the launcher depends in the total initial energy stored in the capacitor bank.

TABLE I
Studded LIL Parameters

Name	Value	Unit
Section one:		
Length (τ)	20	cm
Axial length of coil	3	cm
Average radius	3.425	cm
Radial thickness of coil	1.5	cm
Number of coil	6 (15 turns/coil)	-
Section two:		
length (2τ)	40	cm
Axial length of coil	3	cm
Average radius	3.175	cm
Radial thickness of coil	1	cm
Number of coil	12 (10 turns/coil)	-
Sleeve:		
length (2τ)	20	cm
Average radius	2.5	cm
Radial thickness of coil	1.5	mm
Weight	127g	-
Material	Aluminum	-

A. *Starting section*

The starting section consists of six drive coils spanning one full wave length (20 cm) and is connected in a three-phase configuration. Each phase is energized with a separate capacitor. A total of 14.5 kJ is initially stored in the three-phase capacitors, with different voltages on each. This was necessary in order to achieve equal-amplitude currents in each of the phase windings. Otherwise the delay in firing phases B and C and the asymmetrical mutual inductances between phases result in unequal current amplitudes. The length of the aluminium sleeve equals the length of this section (or one wave length); the thickness is 1.5mm and the weight is 127g. Initially, the left end of the sleeve is positioned at the left end of the barrel.

The mutual inductances among all of the drive and projectile coils are calculated during each incremental movement of the projectile [13]. The method provides results for the mutual inductances between phases winding in the starting section with a first left single projectile ring; coil phase current; velocity; mechanical forces acting on the projectile; and sleeve current.

Fig.3 shows the mutual inductances between phases winding in the starting section with a first left single projectile ring and there gradients dM/dz. When the centre of the coil and the ring are aligned, there is no axial force because the change in mutual inductance is zero.

The dependence of the three phase currents on time is shown in Fig. 4. Phase A is switched on at t = 0, then 60^0 later phase C with a negative initial voltage, and then phase B follows 60^0 after phase C.

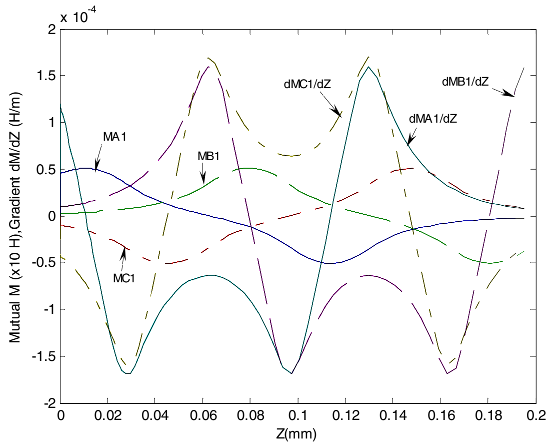

Fig. 3 Mutual inductances and there gradients in the starting section

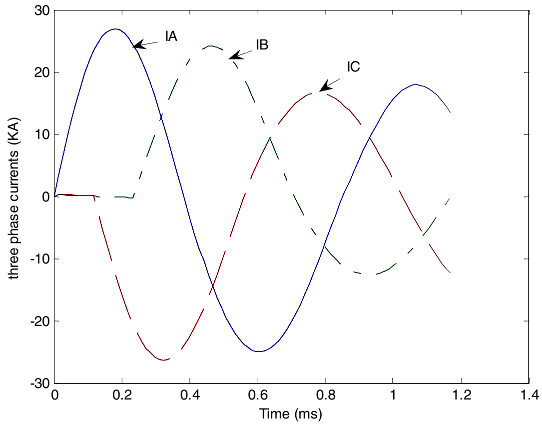

Fig. 4 Three phase currents in the starting section.

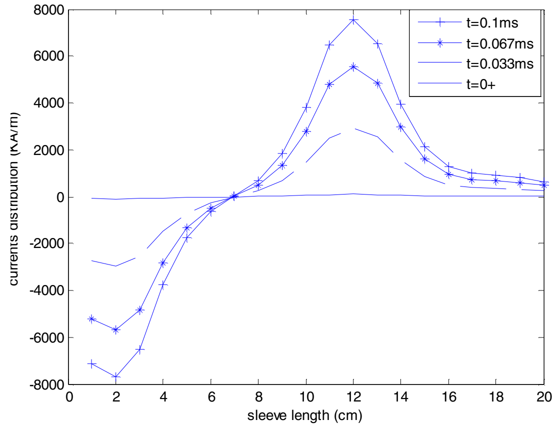

(a)

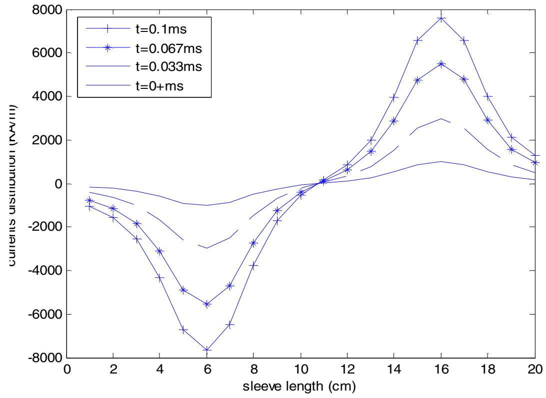

(b)

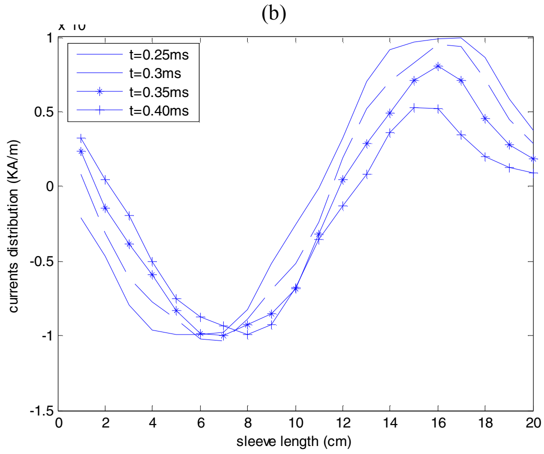

(c)

Fig.5 Sleeve current in the starting section.
(a)- Only phase A is energized. Left end of sleeve coincides with left end of barrel.
(b)- Only phase A is energized, but sleeve is initially placed 5 cm to the left.
(c)- All three-phase windings have been energized. Sleeve is moved 5 cm to the right.

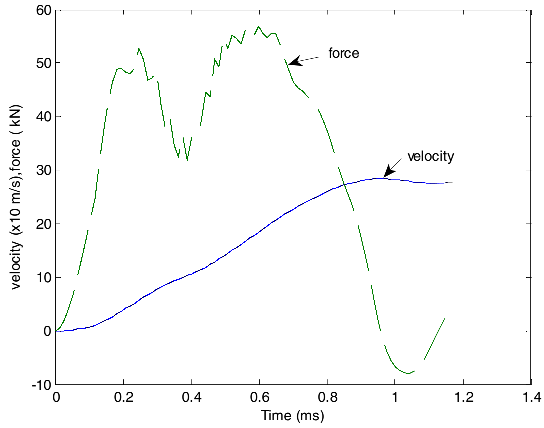

Fig. 6 Force and velocity profiles in the starting section

The frequency and phase-shift variations are caused by asymmetries in the mutual inductances between the phases due to the shortness of the section.

The currents induced in the sleeve are shown in Fig.5 for different configurations. Fig. 5-a shows the current distributions in the sleeve at time: t = 0^{+}, 0.033, 0.067, and 0.1 ms with only phase A is switched on (phase C and B will be switched on at t = 0.12 and 0.24 ms, respectively). Asymmetries in the induced current distribution along the sleeve, as shown in Fig. 5(a), disappear when the sleeve is initially placed at 5 cm to the left of the initial position as compared with Fig. 5(b). The distribution of the sleeve currents after all three-phase windings are energized is shown in Fig. 5-c.

The distorting travelling wave is caused by the space harmonics of the drive coils. Nevertheless, a relatively smooth acceleration is achieved in the first section, as shown in Fig. 6. The projectile accelerates in the first section of the barrel from an initial velocity of zero up to 278 m/s.

For the 14.5 kJ initially stored in the capacitors, 33.85% has been transferred into kinetic energy at exit from the section.

B. Section-to-Section Transition

A smooth transition from one section to the next can be obtained only when the phase shift between the travelling waves generated by the currents in the drive and projectile coils is maintained at a constant level. However, in a capacitively driven coil launcher, a travelling wave cannot be formed until all the three-phase windings of the section are fully energized. For a brief interval of time during the transition, the leading section is single phased. This may result in a change of sign in the accelerating force during the transition and may lead to instability. However, it is possible to alleviate the problem and to achieve a relatively smooth transition from one section to the next by carefully selecting the phase relations in the currents flowing in the dive coils of the two sections.

The currents, force and velocity for the two sections are shown respectively in Fig. 7 and 8. The wave shapes of currents can be improved if the length of the second section is increased. The force on the sleeve (Fig.8) is relatively smooth within a section, but the transition introduced a slightly negative force.

C. Effect of the initial position in the second section

The simulation results for the muzzle velocities are shown in Table II. Again, a wide variation in the initial conditions does not result in a great variation in the muzzle velocity.

TABLE II

MUZZLE VELOCITY V_S. INITIAL POSITION IN THE SECOND SECTION

z_0 [cm]	-4	-3	-2	0	2	3	4
Vs [m/s]	526	539	543	544	528	527	526

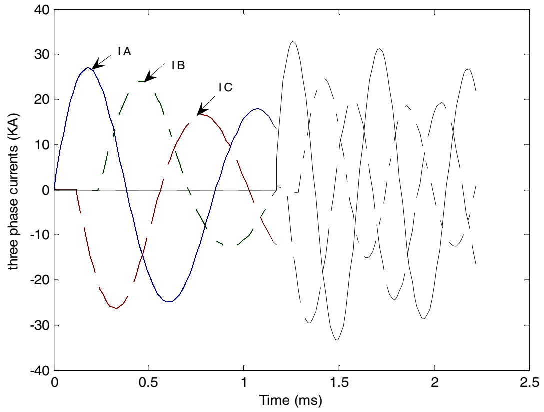

Fig. 7 Tree-phase currents in the two sections

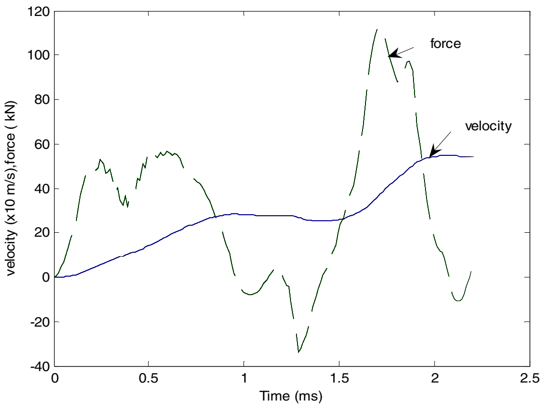

Fig. 8 Force and velocity profiles in two sections.

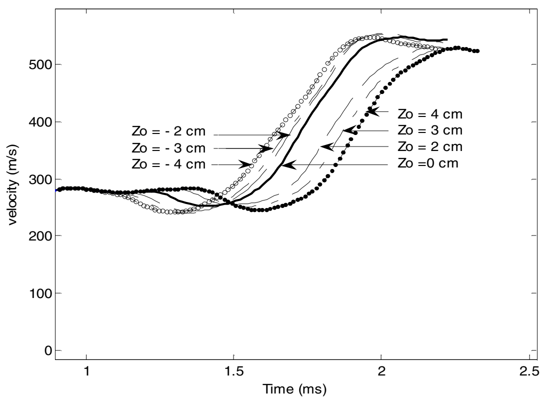

Fig.9. Velocity for different initial positions in the second section.

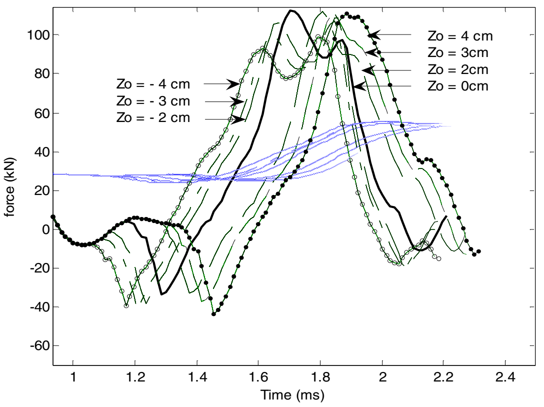

Fig.10. Force for different initial positions in the second section.

Next, the projectile velocities and forces during transit are considered. Fig. 9 and 10 show respectively the velocity and force evolutions in the time for different initial positions in the second section. The best muzzle velocity of 544 m/s is reached at initial position of 0 cm. In the other hand, the smoothest acceleration is obtained with the initial position of -4 cm. This is because the projectile does not get completely into the second section, until the traveling wave is built up. The velocity is only 526 m/s; i.e. less energy is transferred to the sleeve because the decay of the barrel current is fairly rapid. For initial positions -3 and -2 cm, there is a negative force at the beginning until the traveling wave is built up. An explanation is that this negative force is due to mismatch in the phases of the currents in the barrel and in the projectile. For 0 cm initial position, the force due to transformer action by the end effect adds to the motion- induced force. With an initial position of 2, 3 and 4 cm, the latter force becomes stronger.

IV. CONCLUSION

A circuit mesh method based on current filament model, is developed to predicting the two sections linear induction launcher performances powered by bank capacitors. The variation of mutual inductances and his gradient, necessary for this model, with projectile displacement are investigated. The results obtained with this model (currents in the barrel, induced currents in the projectile, force and velocity) shows that the LIL works independently in each section, because the induced currents in the projectile by the previous section are much reduced after leaving a section.

The main factors affecting the transition between sections are the initial velocity and position of the projectile in the second section. However, the LIL performances are relatively insensitive to these factors. The ideal time to fire the next section is when the projectile is completely outside of the previous section. The velocity dip and braking force in transition phase can be minimized by choosing the initial position of the projectile and the next section switch-on time.

V. REFERENCES

[1] J.L.He, E. Levi, Z, Zabar, and L. Birenbaum, ”Transient performance of linear induction launchers fed by generators and by capacitor banks,”*IEEE transactions on magnetics*, vol. 27, No. 1, January 1991.

[2] Z. Zabar, X.N.Lu, E. Levi, Birenbaum, and J. Creedon, ”Experimental results and performance analysis of a 500 m/sec linear induction launcher (LIL),” *IEEE transactions on magnetics*, vol. 31, No. 1, January 1995.

[3] Z. Zabar, Y.Naot, L. Birenbaum, E. Levi and P.N. Joshi, ” Design and power conditioning for the coil-gun,”*IEEE transactions on magnetics*, vol. 25, No. 1, January 1989.

[4] B. Azzerboni, E.Cardilli, M. Raugi, ”A network mesh model for flux compression generators analysis,” *IEEE transactions on magnetics*, vol. 27, No. 5, September 1991.

[5] T. J. Burgess, E. C. Cnare, W. L. Oberkamph, S. G. Beaard and M. Cowan, «The electromagnetic ɵ gun and tubular projectiles”, *IEEE transactions on magnetics*, vol. Mag-18, No. 1, January 1982.

[6] J.L.He, E. Levi, Z, Zabar, and L. Birenbaum, “Analysis of generator-driven linear induction launchers,”*IEEE transactions on magnetics*, vol. 33, No. 1, January 1997.

[7] M.S. Aubuchon, T.R. Lokner, R.J. Kaye, B.N. Turman, “Study of coilgun performance and comments on powered armatures”, Power Modulator Symposium and High-Voltage Workshop, 23-26 May 2004.

[8] J. L He., E. Levi, Z. Zabar, L. Birenbaum and Y. Naot, “Analysis of induction-type coil-gun performance based on cylindrical current sheet model,” *IEEE Transactions on magnetics*, vol. 27, no. 1, pp. 579-584, Jan.1991.

[9] Giancarlo Becherini, “Gyroscopic stabilization of launch package in induction type coilgun,” *IEEE Transactions on magnetics*, vol. 37, no. 1, January 2001.

[10] Jianliang He, Enrico Levi, Zivan Zabar and Leo Birenbaum, "Concering the design of capacitively driven induction coil guns," *IEEE Transactions on magnetics*, vol. 17, no. 3, pp. 429-438, Jun. 1989.

[11] David G. Elliott, "Mesh-matrix analysis method for electromagnetic launchers," *IEEE Transactions on magnetics*, vol. 25, no. 1, pp. 164-169, Jan. 1989.

[12] F. W. Grover, Inductance Calculation. New York: Dover, 1973.

[13] S. Williamson and P.J Leonard, "Analysis of air-cored tubular induction motors," *IEE proceedings, vol. 33, pt. B, no. 4, July 1986.*